Structure, Vol. 10, 609–618, May, 2002, ©2002 Elsevier Science Ltd. All rights reserved. PII S0969-2126(02)00748-7

The Structure of the Mammalian 20S Proteasome at 2.75 Å Resolution

Masaki Unno,[1] Tsunehiro Mizushima,[1] Yukio Morimoto,[2] Yoshikazu Tomisugi,[3] Keiji Tanaka,[4] Noritake Yasuoka,[2] and Tomitake Tsukihara[1,5]

[1]Institute for Protein Research
Osaka University
3-2 Yamadaoka
Suita, Osaka 565-0871
Japan

[2]Faculty of Science
Himeji Institute of Technology
3-2-1 Kohto
Kamigori, Hyogo 678-1297
Japan

[3]The Pharmaceutical Department
Kumamoto University
5-1 Oehonmach
Kumamoto-city, Kumamoto 862-0973
Japan

[4]The Tokyo Metropolitan Institute of Medical Science
3-18-22 Honkomagome
Bunkyo-ku, Tokyo 113-0021
Japan

Summary

The 20S proteasome is the catalytic portion of the 26S proteasome. Constitutively expressed mammalian 20S proteasomes have three active subunits, β1, β2, and β5, which are replaced in the immunoproteasome by interferon-γ-inducible subunits β1i, β2i, and β5i, respectively. Here we determined the crystal structure of the bovine 20S proteasome at 2.75 Å resolution. The structures of α2, β1, β5, β6, and β7 subunits of the bovine enzyme were different from the yeast enzyme but enabled the bovine proteasome to accommodate either the constitutive or the inducible subunits. A novel N-terminal nucleophile hydrolase activity was proposed for the β7 subunit. We also determined the site of the nuclear localization signals in the molecule. A model of the immunoproteasome was predicted from this constitutive structure.

Introduction

The proteasome, a multisubunit proteolytic complex, is the central enzyme of nonlysosomal protein degradation in both the cytosol and nucleus. It is involved in various biological processes, such as the degradation of misfolded proteins and short-lived regulatory proteins [1], and its proteolytic functions are controlled by the ubiquitin system [2, 3]. In this system, the 26S proteasome breaks down polyubiquitinated substrates into short peptides. The degradation of targeted proteins by the 26S proteasome requires ATP hydrolysis, indicating that the 26S proteasome is a eukaryotic ATP-dependent protease [1, 4]. It is an unusually large multisubunit complex, consisting of a central catalytic 20S proteasome and two terminal regulatory subcomplexes, termed PA700 (alias 19S regulatory complex), which are attached to both ends of the central portion in opposite orientations [5, 6].

The crystal structure of the archaeon *Thermoplasma acidophilum* was determined at 3.4 Å resolution in 1995 [7]. The enzyme has a cylindrical shape and is composed of 28 subunits arranged in a particle as four homoheptameric rings, $\alpha_7\beta_7\beta_7\alpha_7$, with D7 symmetry. In 1997, the 20S proteasome from the yeast *Saccharomyces cerevisiae* was determined at 2.4 Å resolution [8]. It resembles the *T. acidophilum* 20S proteasome in size and shape. However, the yeast 20S proteasome is composed of two copies of 14 different subunits, 7 distinct α-type and 7 distinct β-type subunits. These subunits exhibit a unique location with C2 symmetry.

Proteasomes are members of the N-terminal nucleophile (Ntn)-hydrolases superfamily [9]. Their N-terminal threonine residues are exposed as the nucleophile in peptide bond hydrolysis [7, 10]. In eukaryotic cells, three of the β-type subunits have N-terminal threonine residues, are active, and have specificities determined largely by the nature of their S1 pockets [8]. The three major activities, the peptidylglutamil-hydrolyzing (PGPH), trypsin-like, and chymotrypsin-like activities, have been assigned to the three active subunits of β1, β2, and β5, respectively, based on mutational and crystal structure analysis studies [8, 11].

Mammals have 7 different α and 10 different β proteasome subunit genes [11, 12]. In jawed vertebrates, three additional β subunits, β1i, β2i, and β5i, induced by interferon-γ (IFNγ), a major immunomodulatory cytokine [13–15], are catalytically active and replace the constitutive active subunits β1, β2, and β5, respectively, leading to the formation of the "immunoproteasome," which is responsible for immunological processing of intracellular antigens and enhances generation of ligands for class I molecules of the major histocompatibility (MHC) complex [16–19]. β1i and β5i are encoded by the genes in the MHC class II gene region adjacent to the transporters associated with antigen processing genes, which are involved in the transport of antigenic peptides from the cytosol to the endoplasmic reticulum [20].

In mammalian cells, IFNγ also induces expression of another proteasome activator called PA28 or the 11S regulator (REG) subunits (α and β) [5, 21]. PA28, an activator of the 20S proteasome, associates with the 20S proteasome ATP independently to form a football-like structure [22] and markedly stimulates the activities of various peptidases of the 20S proteasome in vitro. However, unlike the 26S proteasome, it fails to enhance

[5]Correspondence: tsuki@protein.osaka-u.ac.jp

Key words: 20S proteasome; crystal structure analysis; immunoproteasome; mammalian proteasome; structure organization; Ntn-hydrolase

Table 1. Residues Whose Main Chain Structures Were Determined and Those Whose Side Chains Remained as Ala Because of the Poor Electron Density

Subunit Residues in Model/Total Residues	Residues Remaining as Ala in the Model
α1: 2–245/246	K45, D46, K55, D62, E146, K181, K186, F187, D188, E196, R245
α2: 1–233/233	R3, K17, V35, Q51, K52, S53, I54, R59, W138, N139, E140, R142, M162, K175, R176, Y177, L183, L192, L194, K195, F198, E199, Q201, V225, K226
α3: 2–255/261	S13, I36, N51, I52, K54, Q177, Y179, M184, I194, L197, M201, K205, K210, K222, K229, Q230, K231
α4: 2–245/248	V26, I40, V42, L43, E46, K47, K48, S49, V50, L53, Q54, E56, K61, N68, I83, F136, D137, F138, D139, T141, Q146, K157, N159, R163, K166, R169, E170, K174, I181, E182, T183, D185, T187, I188, K189, I192, K193, L195, L196, E197, V198, V199, K204, E207, L208, M211, R212, R213, S216, K218, E223, E224, I225, E226, K227, Y228, V229, I232, E233, K234, E235, K236, E237, E238, N239, E240, K241, K242, K243, Q245
α5: 8–241/241	K86, K197, K192, E208, K209, K231
α6: 4–240/263	K208, K216, D217, E237, E238, P240
α7: 1–245/254	N143, E203, K205, K207, R223, E245
β1: 1–202/205	T201, L202
β2: 1–220/234	K9, K180, K205, K215, Q91[a]
β3: 2–205/205	R48
β4: 1–199/201	K41, R95, E109, K185
β5: 1–201/204	K106, E150, I185
β6: 1–213/213	V6, K45, V161, L166, K200
β7: 1–217/219	R44, K156, E170, K195, S216

[a] Glu91 was replaced by Arg based on the electron density map.

the hydrolysis of large protein substrates with native or denatured structures, even when they are ubiquitinated. In vitro studies showed that PA28 could enhance the generation of antigenic peptides by inducing dual substrate cleavages by the 20S proteasome [23]. Recently, it was found that a "hybrid proteasome," comprising the 20S proteasome flanked by PA28 on one side and PA700 on the other, functions as a new ATP-dependent protease [24–26]. However, the counterpart genes of PA28s are not present in budding yeast [12].

The mammalian 20S proteasomes have special roles in the immune system. To elucidate the structure-function relationships, we have been engaged in X-ray structural analysis of the bovine proteasome. The structural analysis should enhance our understanding of the immunological role of 20S proteasomes. Here we report the crystal structure of the 20S proteasome from the bovine liver at 2.75 Å resolution. Our results showed that the structure of the bovine enzyme is different from that of the yeast and accommodates constitutive subunits or inducible subunits.

Results and Discussion

Crystal Structure Determination

Out of almost 1000 crystals inspected, full data sets for crystals were successfully collected. They were not isomorphous with each other, and their resolution limits were 2.75 Å, 3.2 Å, 3.45 Å, 3.7 Å, 4.0 Å, and 4.3 Å. The crystal with the highest resolution was applied for the present study.

Phases were determined by the molecular replacement method using the yeast 20S proteasome truncated to polyalanine as a search model [27]. Most parts of the electron density map were clear, allowing unambiguous assignment of the side chains, although the clarity of the small parts was poor, and, thus, no side chain structures could be designed. Alanine residues were left for parts with poor electron density (Table 1). The electron densities of some N and C termini were unavailable; therefore, their structural models were not built (Table 1). The final structural model was obtained by iterative modeling and refinement using the program CNS [28] at 2.75 Å resolution (Table 2). Other descriptions of the structural analysis have been written in the separate paper [27].

Comparison of General Architecture and Subunit Structures with the Yeast 20S Proteasome

The overall shape of the bovine 20S proteasome was an elongated cylinder with large central cavities and narrow constrictions. The approximate length and diameter of bovine 20S proteasome were 150 and 115 Å, respectively. The α-type subunits were located at the ends, whereas the β-type subunits formed the two equatorial rings. The general architecture of the 20S proteasome was completely conserved among *T. acidophilum* [7], the yeast [8], and mammals. The arrangement of subunits in the bovine 20S proteasome was identical to that in the yeast 20S proteasome.

All α subunits had a β sandwich structure formed by two five-antiparallel β sheets consisting of strands S1 to S10. The sandwich structure was surrounded by helical layers of helices H1 and H2 on one side and H3, H4, and H5 on the other side, as are those of the *T. acidophilum* and the yeast proteasomes. Every α subunit had a helical structure of H0 at the N-terminal side of S1. Structural differences were identified in each α subunit of the bovine enzyme compared with the corresponding subunit of the yeast proteasome (Figure 1; Table 3).

All β subunits of the bovine proteasome had a β sandwich structure similar to the α subunits consisting of strands of S1–S10, similar to those of *T. acidophilum* proteasomes and the yeast. However, the bovine β-type subunits exhibited structural variations at the N-terminal residues before Thr1 in the numbering system of the *T. acidophilum* proteasome and at the C-terminal residues after S10. While overall structure of each β subunit of

Table 2. Crystallographic Statistics of 20S Proteasome from Bovine Liver

Data Collection	
Source	SPring-8-BL41XU
Wavelength (Å)	1.00
Temperature (K)	100
Space group	$P2_12_12_1$
Cell parameters (Å)	
a	315.7
b	205.9
c	116.0
Resolution (Å)	100–2.75 (2.82–2.75)
Reflections	
Total	733,250
Unique	189,429
Completeness (%)	96.3% (70.0%)
$<I/\sigma>$	5.6 (1.8)
R_{sym}[a]	9.5% (40.6%)
Model Refinement	
R[b] (%)/R_{free}[c] (%)	25.0/29.4
Number of atoms	
Protein	47,546
Solvent and ions	195
Rms bond length (Å)	0.008
Rms bond angles (°)	1.40
Ramachandran plot (%)	
Most favored	83.9
Additional allowed	14.7
Generously allowed	1.2
Disallowed	0.1

[a] $R_{sym} = \Sigma I - <I>|/\Sigma<I>$, where I is the observed intensity and $<I>$ is the average intensity over symmetry equivalent measurements.
[b] $R = \Sigma||F_{obs}| - |F_{calc}||/\Sigma|F_{obs}|$.
[c] R_{free} is the same as R but for a 5% subset of all reflections that were not used in crystallographic refinement.

the bovine enzyme was almost identical to that of the corresponding subunit of the yeast enzyme, local structural differences were detected between corresponding β subunits of the bovine and the yeast enzymes (Figure 2; Table 3). The posttranslational processing of eukaryotic β subunits found in the yeast proteasome was confirmed in the structure of the bovine 20S proteasome. The three active subunits of β1, β2, and β5 had N-terminal residues of Thr, similar to *T. acidophilum* β subunits and the yeast active β subunits. The bovine subunits of β6 and β7 had ten and eight extra N-terminal residues, respectively, than the active subunits in the electron density map. These were partly processed during the structural organization. The bovine β4 subunits preserved the Met residue at the N terminus. The Met residue of the bovine β3 subunit at the N terminus could not be located in the clear electron density map, probably because of its disordered conformation.

Structural Conservation of Ntn-Hydrolase Active Sites

The structure of the Ntn-hydrolase active sites of the bovine proteasome were compared by superimposing functional amino acid residues of Thr1, Glu17, Arg19, Lys33, Ser129, Asp166, Ser169, and Gly170. Rmsds for all atoms of the functional residues of the bovine β1–β2, β1–β5, and β2–β5 were 0.4 Å, 0.3 Å, and 0.4 Å, respectively. The locations of these functional residues in each subunit were well conserved among the active β subunits.

The β ring of the bovine proteasome was superimposed on the β ring of the yeast proteasome by the least square fitting of main chain atoms. Rmsd for all atoms of the functional amino acids of β1, β2, and β5 subunits between the corresponding subunits of the bovine and yeast 20S proteasomes were 0.3 Å, 0.3 Å, and 0.2 Å, respectively, which were significantly smaller than the mean value of 0.8 Å of the main chain atoms of β1, β2, and β5. This indicated that the catalytic sites including the substrate binding regions of β1, β2, and β5 were well conserved between the bovine and yeast proteasomes.

Novel Ntn-Hydrolase Active Site of β7 Subunit

The location of the following functional groups around the N-terminal Thr1 (corresponding to Thr-8 of the yeast β7 subunit) of the bovine β7 satisfied the requirement for the Ntn-hydrolase active sites (Figure 3A) [29]. The N-terminal Thr1 formed a hydrogen bond with Asn104 Oδ. Thr1 Oγ-H formed a hydrogen bond with Asp59 Oδ. Arg91 of β1 formed a salt bridge with Asp56 of β7. An oxyanion hole was formed by the Tyr88 OH of β1 or Arg99 Nη of β7. A water molecule was found near Thr1 and must be replaced by a substrate upon formation of the enzyme-substrate complex (Figure 3B). Although the location of functional groups was different from those of β1, β2, and β5, a reasonable reaction mechanism for substrate hydrolysis was developed (Figure 4) [29]. These structural features suggest that the Thr1 of bovine β7 is a novel Ntn-hydrolase active site.

Further analysis also identified a hollow around this active center, which was much smaller than the S1 pockets of β1, β2, or β5 (Figure 3C). This active site should have a small neutral amino acid-preferring (SNAAP) activity [30].

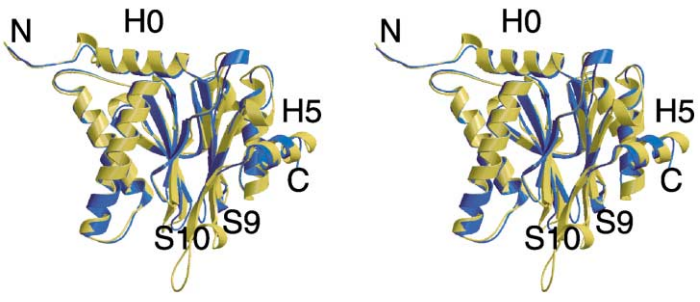

Figure 1. Superposition of the α2 Subunits of the Bovine and Yeast Proteasomes Are Shown by a Stereo Pair

Bovine subunit, blue; yeast subunit, yellow.

Table 3. Main Chain Structures of the Bovine Subunits that Are Different from the Corresponding Yeast Subunits

α1	The N-terminal chain is longer, and the connection between H3 and H4 is shorter.
α2	A turn connects S9 and S10, whereas the yeast subunit has a long insertion forming a loop.
α3	The H5 helix is longer by three turns. The loop structure between S9 and S10 is shorter by two residues.
α4	The bovine and the yeast have different loop structures between S2 and S3.
α5	Both bovine and yeast have long loops between H2 and S5 with a unique conformation at the central part of the α ring, as shown in Figure 7B.
α6	The bovine has a 28-residue longer C terminus. However, C-terminal residues 241–263 are disordered or digested. The H5 helix of the bovine is longer.
α7	The four-residue longer N-terminal region has a different orientation from that of the yeast. The helix H3 is shorter by one turn.
β1	The C terminus is inserted between *trans* β1 and *trans* β7 with a long extended conformation instead of the two-turn helix of the yeast β1 subunit.
β2	No noticeable conformational difference.
β3	No noticeable conformational difference.
β4	The C-terminal region shows extended structure instead of the hooked structure of the yeast β4 subunit.
β5	The bovine terminates in a shorter H5, while the yeast is followed by a C-terminal loop with eight residues.
β6	The loop between H3 and H4 is shorter by eight residues.
β7	The C and N termini are in different orientation from those of the yeast. The loop between H1 and H2 is shorter by four residues.

Thr1 of the bovine β7 subunit was far from the positions of Thr1 of the active subunits of β1, β2, and β5 when they were superimposed by the main chain atoms. The direction of the N-terminal main chain of β7 indicated that the new active site was not in the chamber formed by the two β rings but was close to the gate formed by the α and β rings (Figure 3D).

All the functional groups of Thr1, Asp56, Arg99, and Asn104 of β7 and Tyr88 of β1 were found to be conserved in amino acid sequences of the bovine and yeast enzymes. The three-dimensional locations of these functional groups in both enzymes were similar except for Thr1. The N-terminal threonine of the yeast β7 subunit exhibited a different conformation from the Thr1 of the bovine β7 subunit (Figure 2). Structural comparison of the two structures suggested that the N-terminal chain of yeast β7 can change its conformation to share the novel Ntn-hydrolase active site with the bovine proteasome. However, SNAAP activity has not yet been reported for the yeast enzyme.

Predicted Structure of Immunoproteasome and Substrate Specificities

The sequence identities of the human β1i, β2i, and β5i subunits to the human β1, β2, and β5 were 59.2%, 57.7%, and 68.6%, respectively, while those to the yeast β1, β2, and β5 were 46.0%, 46.0%, and 57.6%, respectively. Any induced subunit of the human 20S proteasome had a higher sequence similarity to the corresponding subunit of the human constitutive proteasome than with that of the yeast. The remaining 11 subunits of the corresponding human constitutive proteasome and the immunoproteasome are identical to each other. Therefore, the X-ray structure of the bovine 20S proteasome was used for more accurate prediction of the three-dimensional structure of the immunoproteasome.

Each S1 pocket of the bovine 20S proteasome was formed by two subunits, as was that of the yeast enzyme [8]. Val20, Phe31, Ser35, and Leu49 of the β1i subunit and His114 and Ser120 of the β2i subunit were located in the S1 pocket of the β1i active site instead of Thr20, Thr31, Thr35, and Arg45 of the β1 subunit and Tyr114 and Asp120 of the β2 subunit. The S1 pocket of β1i was more apolar than that of β1 (Figures 5A and 5B). Thus, it is expected that the PGPH activity would be reduced and chymotryptic activity would be enhanced in the IFNγ-induced 20S proteasome.

In the S1 pockets of β2, no such large structural change was noted upon the introduction of IFNγ-induced subunits (β2i) as was the case of β1i. Ser32 and Asp53 of β2 were replaced by Glus in the β2i subunit. It is conceivable that the trypsin-like activity of the β2i subunit would be enhanced, since the basic residue of the substrate was preferentially located in the pocket (Figure 5C).

At present, there is a general agreement that subunit exchanges induced by IFNγ are likely to confer functional alterations in the immunoproteasome, with increased tryptic and chymotryptic activities of fluorogenic substrates, but reduced PGPH activities for peptides [14, 15, 17], although conflicting results have also been reported on this issue [18, 19]. The present structural model of the immunoproteasome appears to fit with the former observations. In fact, such changes in peptidase activities suggest that the immunoproteasome should generate more peptides that have hydrophobic or basic carboxyl termini and fewer peptides with acidic carboxyl termini. Thus, formation of the immunoproteasome should facilitate the production of MHC class I binding peptides because hydrophobic or basic carboxyl terminal residues normally serve as anchors for binding to MHC class I molecules [17].

KEKE Motifs and Nuclear Localization Signals

The C-terminal helices of the α3 and α4 subunits protruded from the core with high flexibility (Figure 6). These regions contained lysine (K)- and glutamic acid (E)-rich KEKE motifs [6, 31] in the α helices. Interestingly, the C terminus of the α4 subunit in the 20S core particle in *Arabidopsis* can bind an Snf1-related protein kinase (SnRK) in association with the subunit of an Skp1-cullin-F-box (SCF) complex [32]. The C terminus of the human α4 subunit interacts with the hepatitis B virus X protein (HBX) to regulate transcriptional activation of the hepati-

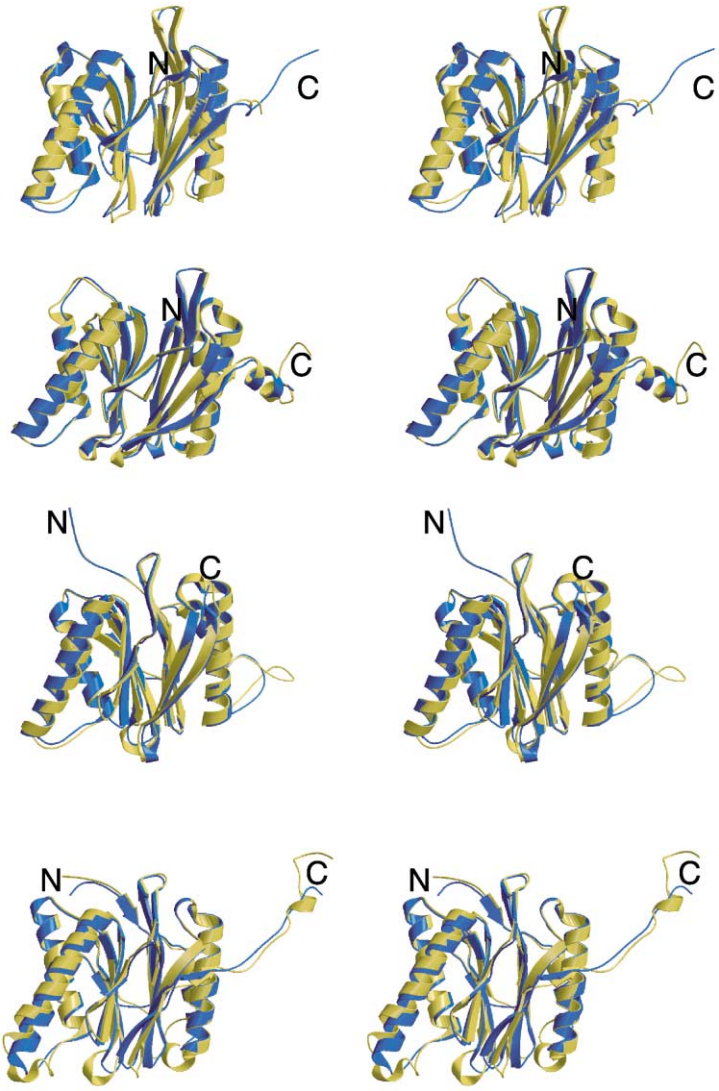

Figure 2. Superposition of the β1, β5, β6, and β7 Subunits (from Top to Bottom) of the Bovine and Yeast Proteasomes Are Drawn as in Figure 1

tis B virus (HBV) [33]. The exposed helical rods with a diameter of about 11–16 Å exhibited a specific charge distribution and seem to interact with the SCF complex and the HBX by ionic interactions.

The consensus sequence X-X-K-K(R)-X-K(R), where X is any residue, has been proposed as the nuclear localization signal (NLS) [34]. The consensus sequences were found in the α1, α2, α3, and α4 subunits. They were Leu-Glu-Lys-Lys-Val-Lys (179–184) in α1, Thr-Glu-Lys-Lys-Gln-Lys (47–52) in α2, Arg-Glu-Lys-Lys-Glu-Lys (249–254) in α3, and Glu-Lys-Lys-Lys-Gln-Lys (240–245) in α4. The residues 179–184 of α1 were in the α helix. The residues 47–52 of α2 were in extended conformations and exhibited high flexibility, judging from their temperature factors. These NLSs were at the surface of the molecule (Figure 6). The NLSs of α3 and α4 were in the C-terminal helices and exhibited high flexibility. These NLS sequences are similar to the basic amino acid cluster motif seen in simian virus 40 (SV40) T antigen. The crystal structure of the complex of importin-α and the NLS peptide of the SV40 T antigen have been reported [35, 36], and the NLS peptide forms an extended conformation. Thus, the NLS of α2 may interact with importin-α, the nuclear import receptors. The importin-α has an internal NLS bounds to its own NLS binding site [37]. The internal NLS changes its conformation from an α helix to an extended conformation upon autoinhibition [37, 38]. These findings suggest that the NLS helices of α1, α3, or α4 may change their conformations to interact with the importin-α. In this context, it is possible that the proteasome is imported to the nucleus by the importin-α.

The Central Pore of the α Ring

The bovine 20S proteasome had no obvious path for the substrate to access the active center chamber because the extreme N termini of the α2, α3, and α4 subunits and the loop structure of α5 subunit filled the central pore, similarly as in the yeast 20S proteasome (Figure 7A). The N-terminal polypeptides of the bovine α subunits, which correspond to the disordered N-terminal regions of the *T. acidophilum* α subunit, had individual tertiary structures with higher temperature factors than their β sandwich core structures, similar to those

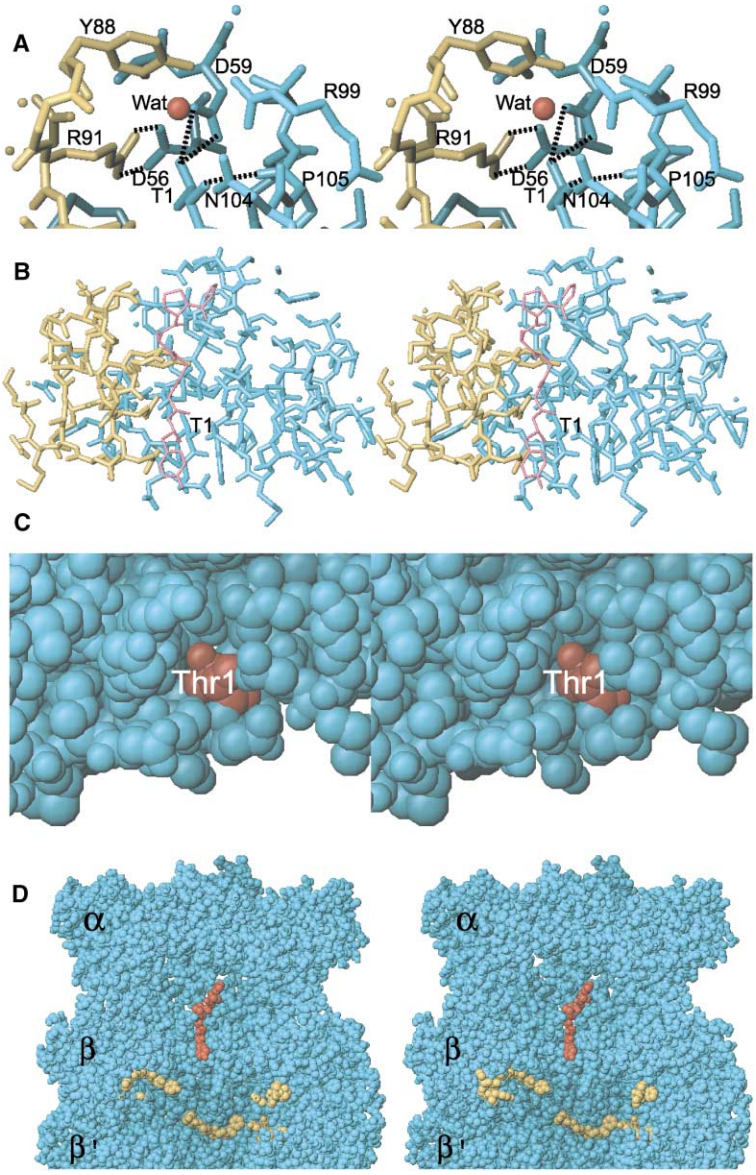

Figure 3. Stereoviews of the New Ntn-Hydrolase Active Site Projected along Almost the Same Directions

(A) Residues included in the catalysis are shown by the single letter notation with the residue number of the bovine subunit. β1 subunit, yellow; β7 subunits, sky blue. The red sphere is a water molecule.

(B) Predicted structure of the model substrate Phe-Gly-Pro-Ala-Gly-Gly-Tyr fitted in the β7 active site. β1 subunit, yellow; β7 subunit, sky blue; model substrate, red.

(C) The active site was drawn by a space-filling model to show its hollow surface. Thr1 (red) is located at the bottom of this hollow.

(D) The predicted substrate structures in the 20S proteasome. The red model is the substrate of the novel β7 active site; the three yellow models are those of β1, β2, and β5 active sites. The α ring, β ring, and *trans* β (β′) ring are depicted in part for convenience. The novel Ntn catalytic site is in a different position and a different orientation (red) from the other three active sites (yellow).

in the yeast α subunit. Both α5S of the bovine and yeast proteasomes had long loops consisting of five and six insertion residues, respectively, between H2 and S5. The loops of the bovine and yeast α5 subunits exhibited individual conformations with high temperature factors at the central part of the α rings. These structural features suggest that the N-terminal residues of the α subunits and the loop of α5 changed their conformations in binding regulatory complexes and upon introduction of a substrate as proposed previously by Groll et al. [8, 39] and Whittby et al. [40].

Interaction across the Rings and Interchange of the Constitutive and Inducible Subunits

The bovine α2 subunit lacked a long loop between the two strands of S9 and S10 of the yeast α2 subunit, which interacts with Asp-Ala-Glu-Tyr (183–186) and Lys40 of the β2 subunit (Figures 1 and 7B). These amino acid residues were equivalent to Lys-Leu-Asp-Phe (182–185) and Asn40 of the constitutive β2 subunit and Gly-Ala-Lys-Leu (182–185) and Lys40 of the induced β2i subunit. The sequences of the three β2 and β2i subunits were completely different. The bovine 20S proteasome can accommodate both β2 and β2i at the same position of the β ring by the deletion of the long loop between S9 and S10 of the yeast α2 subunit.

The mammalian β5 and β5i subunits did not have seven residues present at the C terminus of the yeast β5 subunit, which make close contacts with the *trans* β3 (β3′) and *trans* β4 (β4′) subunits. These specific interactions in the yeast 20S proteasome were not seen in the bovine 20S proteasome structure (Figures 2 and 7C).

The loop between helices H4 and H5 of the bovine β6 subunit was shorter than that of the yeast β6 subunit, which contacts the long C-terminal extensions of *trans* β2 (β2′). The contact was not seen in the bovine enzyme (Figures 2 and 7C).

The C-terminal region of bovine β1, which is sand-

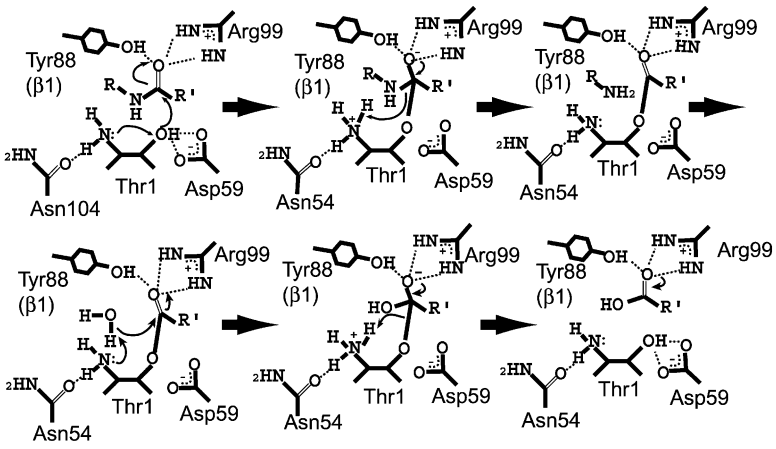

Figure 4. Putative Catalytic Mechanism of the Novel Active Site in β7

The reaction begins when the nucleophilic oxygen of Thr1 donates its proton to its own α-amino group and attacks the carbonyl carbon of the substrate. The negatively charged tetrahedral intermediate is stabilized by hydrogen bonding. The acylation step is complete when the α-amino group of Thr donates a proton to the nitrogen of the scissile peptide bond. The covalent bond between part of the substrate and the enzyme is formed, and the part of the substrate is released. The deacylation step begins when the hydroxyl group of water attacks the carbonyl carbon of the acyl-enzyme product and the basic α-amino group of the nucleophile accepts the proton from the water molecule. The negatively charged intermediate is stabilized, as in the acylation step. The reaction is completed when the α-amino group donates a proton to the nucleophile.

wiched between the *trans* β1 (β1′) and *trans* β7 (β7′) subunits, exhibited a flexible extended conformation with poor intersubunit interactions, such as a few hydrogen bonds (Figures 2 and 7C). Since the C-terminal extension of β1i was expected to have a flexible structure, similar to β1, it could be accommodated between *trans* β1i (β1i′) and β7′.

The long C-terminal regions of bovine β7 and yeast β7 were located between the respective β1′ and β2′ subunits. The yeast β7 C-terminal region with 20 residues has six hydrogen bonds between β7 and β1′ and between β7 and β2′. However, the C-terminal region of bovine β7 with 13 residues had only two hydrogen bonds between β7 and β1′ and between β7 and β2′, and their contacts were loose (Figures 2 and 7C). Thus, the β7 subunit of the bovine enzyme does not prevent β1′ and β2′ from being replaced by β1i′ and β2i′, respectively.

The bovine 20S proteasome exhibited fewer intersubunit interactions for β1, β2, and β5 than the yeast. The bovine β1, β2, and β5 subunits were fixed in the β ring by intersubunit interactions participated by conservative residues between the constitutive and inducible sub-

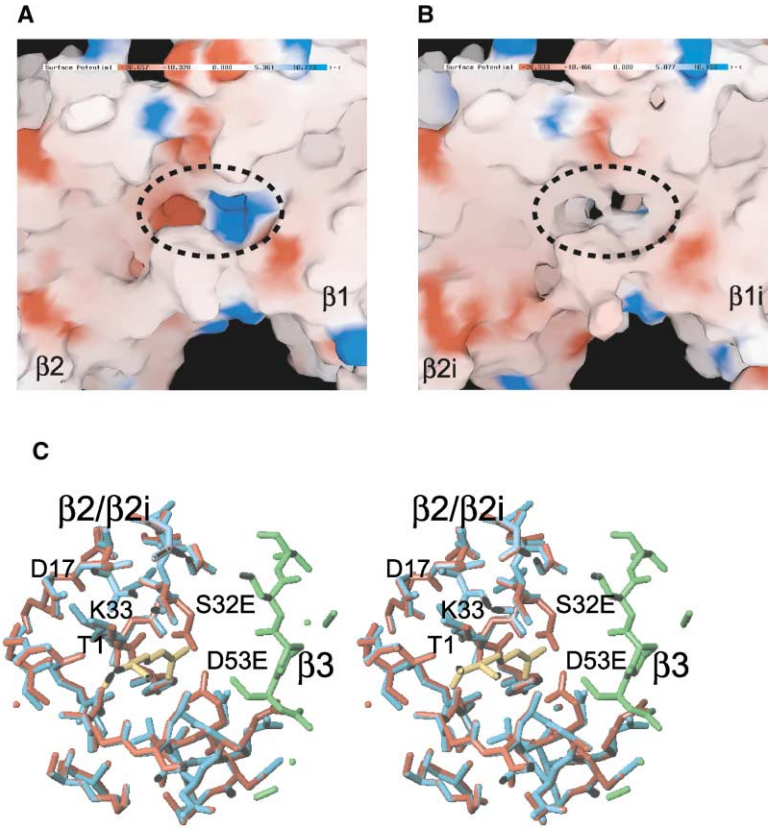

Figure 5. Structure Comparison of the Active Centers of the Constitutive Proteasome with the Active Centers of the Immunoproteasome

(A and B) Diagrams of electrostatic surface potential of S1 pockets for the β1 and β1i active sites. Negative potentials, red; positive potentials, blue. The S1 pocket is surrounded by a dotted circle. The S1 pocket of the β1 active center is formed by both β1 and β2 subunits.

(A) The S1 pocket of the β1 active center is charged positively at the β2 subunit side and negatively at the β1 subunit side.

(B) The S1 pocket of the β1i active center of the immunoproteasome is almost apolar.

(C) Structure comparison of the β2 and β2i active centers in a stereo pair. Amino acid residues are represented by the single letter notations with residue numbers. Both Ser32 and Asp53 in the constitutive subunit β2 (sky blue) are replaced by Glu in inducible subunit β2i (red). The green peptide is part of the β3 subunit, and the yellow peptide is a model substrate.

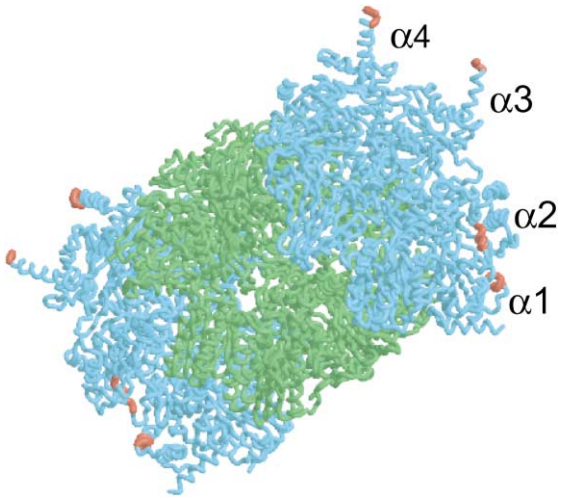

Figure 6. Locations of NLSs in the Bovine 20S Proteasome
α subunits, sky blue; β subunits, green; NLSs, red.

units. Exchange of constitutive and inducible subunits of the mammalian 20S proteasome was achieved by removing extra intersubunit interactions that are recognized only in the yeast proteasome.

Biological Implications

Our X-ray analysis of the structure of the bovine 20S proteasome proved that the yeast proteasome and mammalian proteasome have the same subunit arrangement and showed that the general structural features of eukaryotic 20S proteasome are similar to those of the yeast 20S proteasome. Furthermore, the functional groups of the N-terminal hydrolase active sites were well conserved among the bovine, yeast, and *T. acidophilum* 20S proteasomes [7, 8].

A novel Ntn-hydrolase active site was assigned to the β7 subunit by inspecting the location of functional groups in the molecule. The active site cleft was much shallower than the S1 pockets of β1, β2, and β5 (Figure 3C). The active site may have SNAAP activity.

Several polypeptide segments with NLS were located at the molecular surface (Figure 6). These polypeptide segments are thought to interact with importin-α upon transportation across the nuclear pore.

Substrate specificities of the immunoproteasome predicted from the yeast 20S proteasome structure [8, 19] can also be predicted in the bovine 20S proteasome. In the immunoproteasome, the β1i active site can reduce PGPH activity and can enhance chymotrypsin-like activity, while the β2i active site can enhance trypsin-like

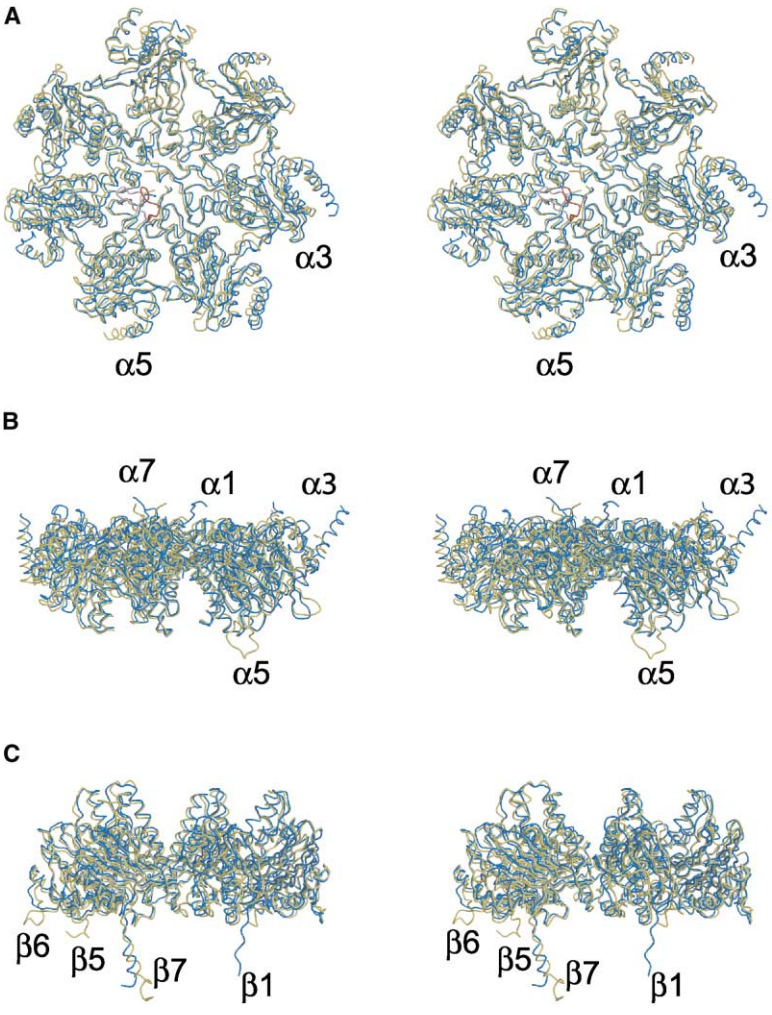

Figure 7. Structural Comparisons of the Bovine α and β Rings with the Yeast α and β Rings Are Shown by Stereoscopic Drawings
Bovine subunits, blue; yeast subunits, yellow. Several subunit names are shown in each drawing.
(A) Top views of the α rings show the structural difference between residues 124–134 of the bovine α5 (red) and the corresponding residues of the yeast α5 subunit (pink).
(B) Side views of the α rings clearly show the structural differences of the α1, α3, α5, and α7 subunits between the bovine and the yeast enzyme. Note that each α ring interacts with a β ring at the bottom.
(C) Side views of the β rings. The bottom side interacts with the β ring related by 2-fold symmetry.

activity. Thus, it seems that the immunoproteasome is more advantageous for producing peptides for antigen presentation to MHC class I molecules.

The bovine proteasome gained the ability to interchange mutually the constitutive subunits and the inducible subunits by losing several intersubunit interactions detected in the yeast proteasome.

Experimental Procedures

X-ray diffraction experiments and structure determination were described in the separate paper [27].

Structural Predictions of the Immunoproteasome and Substrate Binding Models

An initial model of the immunoproteasome was constructed by exchanging the residues of constitutive subunits with those of the inducible subunits, with their standard side chain conformations taken from the dictionary of TURBO-FRODO [41]. The initial model was refined by positional refinement using X-PLOR [42]. In this step, the remaining constitutive subunits were fixed and water molecules were excluded. The electrostatic surface potential was calculated and displayed using GRASP [43]. The structural model of Phe-Gly-Pro-Ala-Gly-Gly-Tyr at the active site of the β7 subunit (Figures 3B and 3D), the structural model of Phe-Gly-Pro-Ala-Leu-Gly-Tyr at the β1, β2, and β5 subunits (Figure 3D), and the structural model of Phe-Ala-Ala-Arg-Trp at the β2 and β2i (Figure 5C) were constructed as follows. Initial models of these peptides were built as extended forms and fitted to the proper positions within the enzyme molecule. Then, their conformations were changed manually to reduce the interatomic repulsion of protein using TURBO-FRODO [41]. The final models were obtained by positional refinement coupled with simulated annealing using X-PLOR [42]. In this calculation, the atomic parameters of the protein molecule were fixed, and only those of the model peptides were refined.

Amino Acid Sequences

Because the amino acid sequences of the bovine proteasome were unknown, the amino acid sequences of the human proteasome were substituted for those of the bovine enzyme. Since the amino acid sequences of the human and rat 20S proteasomes show 98.5% homology, those of the bovine enzyme must have higher similarity to the human enzyme than the rat enzyme. The amino acid sequences of the yeast and human proteasomes were taken from SWISSPROT. The N-terminal residue of any subunit was assigned as a first residue for the bovine 20S proteasome. Thus, the numbering system was different from that of the yeast β-type subunits [8]. Primary structure alignments among the subunits were conducted using CLUSTALW [44].

Acknowledgments

We thank N. Kamiya and M. Kawamoto at SPring-8 (BL41XU). This work was partly supported by Grants-in-Aid for JSPS Fellows to M.U. from the Ministry of Education, Science, Sports, and Culture, by a Grant-in-Aid for "Research for the Future" Program from the Japan Society for the Promotion of Science (JSPS-RFTF96L00503 to T.T.), and by Grants-in-Aid for Scientific Research on Priority Area (10188101 and 10179101 to T.T.). This research was conducted with prior approval of SPring-8, the Institute of Physical and Chemical Research (RIKEN), the Institute for Protein Research (Proposal 2000B0083-NL-np and 1999A0377-NL-np for BL41XU and C01A44XU-7143-N and C01B44XU-7143-N for BL44XU), the Photon Factory Advisory Committee, and the National Laboratory for High Energy Physics, Japan (Proposal 98G-149).

Received: October 30, 2001
Revised: February 15, 2002
Accepted: February 22, 2002

References

1. Coux, O., Tanaka, K., and Goldberg, A.L. (1996). Structure and functions of the 20S and 26S proteasomes. Annu. Rev. Biochem. *65*, 801–847.
2. Hershko, A., and Ciechanover, A. (1998). The ubiquitin system. Annu. Rev. Biochem. *67*, 425–479.
3. Pickart, C.M. (2001). Mechanisms underlying ubiquitination. Annu. Rev. Biochem. *70*, 503–533.
4. Baumeister, W., Walz, J., Zuhl, F., and Seemuler, E. (1998). The proteasome: paradigm of a self-compartmentalizing protease. Cell *92*, 367–380.
5. DeMartino, G.N., and Slaughter, C.A. (1999). The proteasome, a novel protease regulated by multiple mechanisms. J. Biol. Chem. *274*, 22123–22126.
6. Voges, D., Zwickl, P., and Baumeister, W. (1999). The 26S proteasome, a molecular machine designed for controlled proteolysis. Annu. Rev. Biochem. *68*, 1015–1068.
7. Löwe, J., Stock, D., Jap, B., Zwickl, P., Baumeister, W., and Huber, R. (1995). Crystal structure of the 20S proteasome from the archaeon *T. acidophilum* at 3.4 Å resolution. Science *268*, 533–539.
8. Groll, M., Ditzel, L., Lowe, J., Stock, D., Bochtler, M., Bartunik, H.D., and Huber, R. (1997). Structure of 20S proteasome from yeast at 2.4 Å resolution. Nature *386*, 463–471.
9. Brannigan, J.A., Dodson, G., Duggleby, H.J., Moody, P.C., Smith, J.L., Tomchick, D.R., and Murzin, A.G. (1995). A protein catalytic framework with an N-terminal nucleophile is capable of self-activation. Nature *378*, 416–419.
10. Seemüller, E., Lupas, A., and Baumeister, W. (1996). Autocatalytic processing of the 20S proteasome. Nature *382*, 468–472.
11. Bochtler, M., Ditzel, L., Groll, M., Hartmann, C., and Huber, R. (1999). The proteasome. Annu. Rev. Biophys. Biomol. Struct. *28*, 295–317.
12. Tanaka, K. (1998). Molecular biology of the proteasome. Biochem. Biophys. Res. Commun. *247*, 537–541.
13. Monaco, J.J., and Nandi, D. (1995). The genetics of proteasomes and antigen processing. Annu. Rev. Genet. *29*, 729–754.
14. Tanaka, K., and Kasahara, M. (1998). The MHC class I ligand-generating system: roles of immunoproteasomes and the interferon-γ-inducible proteasome activator PA28. Immunol. Rev. *163*, 161–176.
15. Fruh, K., and Yang, Y. (1999). Antigen processing by MHC class I and its regulation by interferon γ. Curr. Opin. Immunol. *11*, 76–81.
16. Pamer, E., and Cresswell, P. (1998). Mechanisms of MHC class I-restricted antigen processing. Annu. Rev. Immunol. *16*, 323–358.
17. Rock, K.L., and Goldberg, A.L. (1999). Degradation of cell proteins and the generation of MHC class I-presented peptides. Annu. Rev. Immunol. *17*, 739–779.
18. Niedermann, G., Geier, E., Lucchiari-Hartz, M., Hitziger, N., Ramsperger, A., and Eichmann, K. (1999). The specificity of proteasomes: impact on MHC class I processing and presentation of antigens. Immunol. Rev. *172*, 29–48.
19. Kloetzel, P.M. (2001). Antigen processing by the proteasome. Nat. Rev. Mol. Cell Biol. *2*, 179–187.
20. Flajnik, M.F., and Kasahara, M. (2001). Comparative genomics of the MHC: glimpses into the evolution of the adaptive immune system. Immunity *15*, 351–362.
21. Rechsteiner, M., Realini, C., and Ustrell, V. (2000). The proteasome activator 11S REG (PA28) and class I antigen presentation. Biochem. J. *345*, 1–15.
22. Gray, C.W., Slaughter, C.A., and DeMartino, G.N. (1994). PA28 activator protein forms regulatory caps on proteasome stacked rings. J. Mol. Biol. *236*, 7–15.
23. Dick, T.P., Ruppert, T., Groettrup, M., Kloetzel, P.M., Kuehn, L., Koszinowski, U.H., Stevanovic, S., Schild, H., and Rammensee, H.G. (1996). Coordinated dual cleavages induced by the proteasome regulator PA28 lead to dominant MHC ligands. Cell *86*, 253–262.
24. Tanahashi, N., Murakami, Y., Minami, Y., Shimbara, N., Hendil, K.B., and Tanaka, K. (2000). Hybrid proteasomes: induction by interferon-γ and contribution to the ATP-dependent proteolysis. J. Biol. Chem. *275*, 14336–14345.

25. Kopp, F., Dahlmann, B., and Kuehn, L. (2001). Reconstitution of hybrid proteasomes from purified PA700-20S complexes and PA28alphabeta activator: ultrastructure and peptidase activities. J. Mol. Biol. *313*, 465–471.
26. Hendil, K.B., Khan, S., and Tanaka, K. (1998). Simultaneous binding of PA28 and PA700 activators to 20S proteasomes. Biochem. J. *332*, 749–754.
27. Unno, M., Mizushima, T., Morimoto, Y., Tomisugi, Y., Tanaka, K., Yasuoka, N., and Tsukihara, T. (2002). Structure determination of the constitutive 20S proteasome from bovine liver at 2.75 Å resolution. J. Biochem. (Tokyo) *131*, 171–173.
28. Brunger, A.T., Adams, P.D., Clore, G.M., DeLano, W.L., Gros, P., Grosse-Kunstleve, R.W., Jiang, J.S., Kuszewski, J., Nilges, M., Pannu, N.S., et al. (1998). Crystallography and NMR system: a new software suite for macromolecular structure determination. Acta Crystallogr. D Biol. Crystallogr. *54*, 905–921.
29. Oinonen, C., and Rouvinen, J. (2000). Structural comparison of Ntn-hydrolase. Protein Sci. *9*, 2329–2337.
30. Orlowski, M., Cardozo, C., and Michaud, C. (1993). Evidence for the presence of five distinct proteolytic components cleaving in the pituitary multicatalytic proteinase complex. Properties of two components cleaving bonds on the carboxyl side of branched chain and small neutral amino acids. Biochemistry *32*, 1563–1572.
31. Realini, C., Roberts, S.W., and Rechsteiner, M. (1994). KEKE motifs: proposed roles in protein-proteon association and presentation of peptides by MHC class I receptors. FEBS Lett. *348*, 109–113.
32. Farras, R., Ferrando, A., Jasik, J., Kleinow, T., Okresz, L., Tiburcio, A., Salchert, K., del Pozo, C., Schell, J., and Koncz, C. (2001). SKP1-SnRK protein kinase interactions mediate proteasomal binding of plant SCF ubiquitin ligase. EMBO J. *20*, 2742–2756.
33. Huang, J., Kwong, J., Sun, E.C.-Y., and Liang, T.J. (1996). Proteasome complex as a potential cellular target of hepatitis B virus X protein. J. Virol. *70*, 5582–5591.
34. Roberts, B. (1989). Nuclear location signal-mediated protein transport. Biochim. Biophys. Acta *1008*, 263–280.
35. Fontes, M.R., The, T., and Kobe, B. (2000). Structural basis of recognition of monopartite and bipartite nuclear localization sequences by mammalian importin-α. J. Mol. Biol. *297*, 1183–1194.
36. Conti, E., and Kuriyan, J. (2000). Crystallographic analysis of the specific yet versatile recognition of distinct nuclear localization signals by karyopherin α. Structure *8*, 329–338.
37. Kobe, B. (1999). Autoinhibition by an internal nuclear localization signal revealed by the crystal structure of mammalian importin α. Nat. Struct. Biol. *6*, 388–397.
38. Cingolani, G., Petosa, C., Weis, K., and Müller, C.W. (1999). Structure of importin–β bound to the IBB domain of importin-α. Nature *399*, 221–229.
39. Groll, M., Bajorek, M., Kohler, A., Moroder, L., Rubin, D.M., Huber, R., Glickman, M.H., and Finley, D. (2000). A gated channel into the proteasome core particle. Nat. Struct. Biol. *7*, 1062–1067.
40. Whitby, F.G., Masters, E.I., Kramer, L., Knowlton, J.R., Yao, Y., Wang, C.C., and Hill, C.P. (2000). Structural basis for the activation of 20S proteasome by 11S regulators. Nature *408*, 115–120.
41. Jones, T.A. (1978). A graphics model building and refinement system for macromolecules. J. Appl. Crystallogr. *11*, 268–272.
42. Brünger, A.T. (1992). X-PLOR Version 3.1. A System for X-Ray Crystallography and NMR (New Haven, CT: Yale University Press).
43. Nicholls, A., Sharp, K.A., and Honing, B. (1991). Protein folding and association: insights from the interfacial and thermodynamic properties of hydrocarbons. Proteins *11*, 281–296.
44. Thompson, J.D., Higgins, D.G., and Gibson, T.J. (1994). CLUSTAL W: improving the sensitivity of progressive multiple sequence alignment through sequence weighting, position-specific gap penalties and weight matrix choice. Nucleic Acids Res. *22*, 4673–4680.

Accession Numbers

The atomic parameters and structure factors have been deposited in the Protein Data Bank with the accession codes 1IRU and rIRUsf.ent, respectively.